Techniques for Diffusion Tensor Imaging in Mouse Brain

Jiang-yang Zhang, Ph.D.
Assistant Professor of Radiology
Division of NMR research
Russell H. Morgan Department of Radiology and Radiological Sciences
Johns Hopkins University School of Medicine

Introduction

In neuroscience research, mouse models have played important roles in advancing our knowledge of the brain and its diseases. To study mouse neuroanatomy, especially changes in neuroanatomy caused by genetic mutation or pathology, novel imaging tools are necessary. Diffusion tensor imaging (DTI) is a good candidate because it can visualize white matter (WM) structures in the brain, and has been used to study neurological diseases, such as multiple sclerosis and Alzheimer's disease.

Even though DTI has been routinely performed in the clinic, DTI of the mouse brain remains a challenging task. A mouse brain is approximately 1000 times smaller than a human brain in term of the total volume. The current resolution of human brain DTI is about 1 - 2 mm per pixel. In order to achieve the same relative resolution, we need to achieve a resolution of 0.1 - 0.2 mm per pixel for mouse brain DTI by using special techniques.

Technical challenges of mouse brain DTI

The primary technical challenge in DTI of the mouse brain is to achieve high spatial resolution while preserving satisfactory signal to noise ratio (SNR). DTI is known as a poor SNR technique because the signal magnitude in diffusion weighted images is attenuated by diffusion sensitizing gradients. To achieve satisfactory SNR, most mouse brain DTI experiments have been performed on high field systems with custom made coils. The disadvantage of strong magnetic field is that it shortens tissue T_2 while lengthen tissue T_1. High field systems also have more severe field inhomogeneity than 1.5 Tesla or 3 Tesla magnets. The short T_2 and field inhomogeneity make implementation of echo planar imaging (EPI) type of acquisition, commonly used for clinical DTI, difficult on high field systems. In addition to the resolution challenge, DTI data are often marred by artifacts caused by subject motion or gradient eddy current. Subject motion during *in vivo* experiment can be minimized by better animal constrains and respiratory triggering. Eddy current artifact can be significantly reduced by adjusting the gradient pre-emphasis.

Even with these challenges, DTI of mouse brain has many advances in recent years. Table 1 lists several DTI experiments and their imaging parameters. The best resolution achieved for *in vivo* DTI is approximately 0.1 mm x 0.1 mm x 0.5 mm [1], and the best resolution achieved for *ex vivo* DTI is 0.02 mm x 0.02 mm x 0.3 mm [2].

Applications	**Resolution and imaging parameters**
Budde, M.D. et al. [1] Axon and myelin injury in the mouse spinal cords in experimental autoimmune encephalomyelitis	0.078 mm x 0.078 mm x 1 mm, in vivo, 4.7 Tesla spectrometer, spin echo, Δ=25 ms, δ = 10 ms, b = 785 s/mm^2. Total imaging time = 2 hours
Sun, S.W. et al. [3] Axon and myelin degeneration in the mouse brains	0.117 mm x 0.117 mm x 0.5 mm, in vivo, 4.7 Tesla spectrometer, spin echo, Δ =25 ms, δ = 10 ms, b = 768 s/mm^2. Total imaging time = 3 hours
Sizonenko, S.V. et al. [4] Early cortical injury in neonatal rat after hypoxic ischemic injury	0.125 mm x 0.125 mm x 0.5 mm, in vivo, 4.7 Tesla spectrometer, spin echo, Δ =25 ms, δ = 10 ms, b = 768 s/mm^2. Total imaging time = 4 hours
Ahren, E.T. et al. [2] axon and myelin pathology in the mouse spinal cords in spontaneously acquired	0.02 mm x 0.02 mm x 0.3 mm, ex vivo, 11.7 Tesla spectrometer, spin echo, Δ = 7.4 ms, δ = 2

experimental allergic encephalomyelitis	ms, b = 2000 s/mm^2.
Tyszka, J.M. [5] white matter abnormalities in myelin deficit shiverer mouse brains	0.08 mm x 0.08 mm x 0.08 mm, ex vivo, 11.7 Tesla spectrometer, spin echo, Δ = 5 ms, δ = 3 ms, b = 1450 s/mm^2.
Mori et al. [6], Zhang, J. et al. [7] Cortical and white matter development in embryonic mouse brains	0.08 mm x 0.08 mm x 0.08 mm, ex vivo, 9.4 Tesla spectrometer, spin echo, Δ =12 ms, δ = 5 ms, b = 1200 s/mm^2. Total imaging time = 24 hours

Table 1: *Selected DTI studies of mouse and rat brain or spinal cord. Note that the diffusion times (Δ) in these experiments (~ 10 ms) are much shorter than in clinical DTI (~80 ms) because of the short T_2 in high field.*

Pulse sequences for mouse brain DTI

Typical DTI pulse sequence consists of two parts: diffusion preparation and signal acquisition. For the preparation part, most DTI experiments use spin echo preparation (Fig. 1A) because stimulated echo preparation (Fig. 1B) reduces SNR by 50% if ignoring the effect of T_2 decay. However, if a long diffusion time (e.g. 80 ms) is necessary, stimulated echo preparation should be used. To reduce eddy current related imaging artifacts, double refocusing bipolar diffusion gradient, which employs two refocusing pulses and two pairs of diffusion gradients with opposite polarities, can be used (Fig. 1C) [8]. With bipolar gradients, the eddy current induced by the first diffusion gradient will be cancelled by the eddy current induced by the second, opposite diffusion gradient. In practice, this scheme can significantly reduce eddy current artifacts. However, the additional refocusing pulse in this scheme reduces SNR and increases the complexity of pathway selection for multiple echo acquisition.

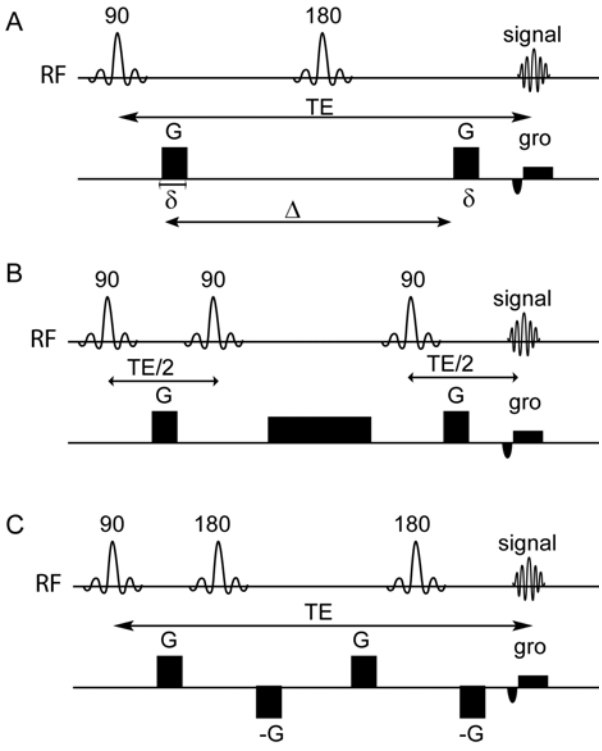

Figure 1: *Spin echo (A), stimulated echo (B), and double refocusing bipolar gradient (C) diffusion preparation. In the bipolar gradient preparation, two refocusing pulses follow the initial excitation pulse. Pairs of diffusion gradients with opposite polarity are positioned around each refocusing pulse to reduce diffusion gradient induced eddy current.*

For the acquisition part, most mouse brain DTI experiments avoid EPI acquisition due to the artifacts associated with EPI based acquisition on high field system. A diagram of a diffusion weighted spin echo sequence is shown in Figure 2. To achieve better resolution and SNR, users can choose from two spin echo based approaches: multiple spin echo (MSE) and fast spin echo (FSE). In both cases, the number of echoes that can be acquired is limited by the T_2 decay. In the MSE experiments, multiple images are acquired and added together to enhance SNR. Choice of FSE or MSE acquisition depends on imaging time, resolution, and SNR requirements. FSE is more time efficient, and is well-suited for *in vivo* experiments. MSE requires the same amount of time as the conventional spin echo sequence, but produces better SNR due to the additional signal averaging. In both MSE and FSE acquisitions, unwanted coherence pathways can rise from imperfect refocusing pulses. These coherence pathways are not encoded properly by diffusion and phase encoding gradients, and can cause artifacts in the reconstructed images. It is necessary to combine phase cycling with crusher gradients around the refocusing pulses to remove these unwanted coherence pathways. For FSE

acquisition, phase differences between even and odd echoes can cause severe artifacts in the reconstructed images (Fig. 2). However, if the crusher gradients are selected properly to remove all unwanted coherence pathways, the phase differences between odd and even echoes are constant. This enables the use of twin-navigator echo correction scheme (Fig. 2) to remove the phase differences [9]. In this scheme, two additional navigator echoes are positioned at the end of the echo trains. One navigator echo records the phase of the odd echoes and the other one records the phase of the even echoes. During image reconstruction, the phase difference information from the navigator echoes can be used to remove phase incoherence in the *k*-space and related image artifacts.

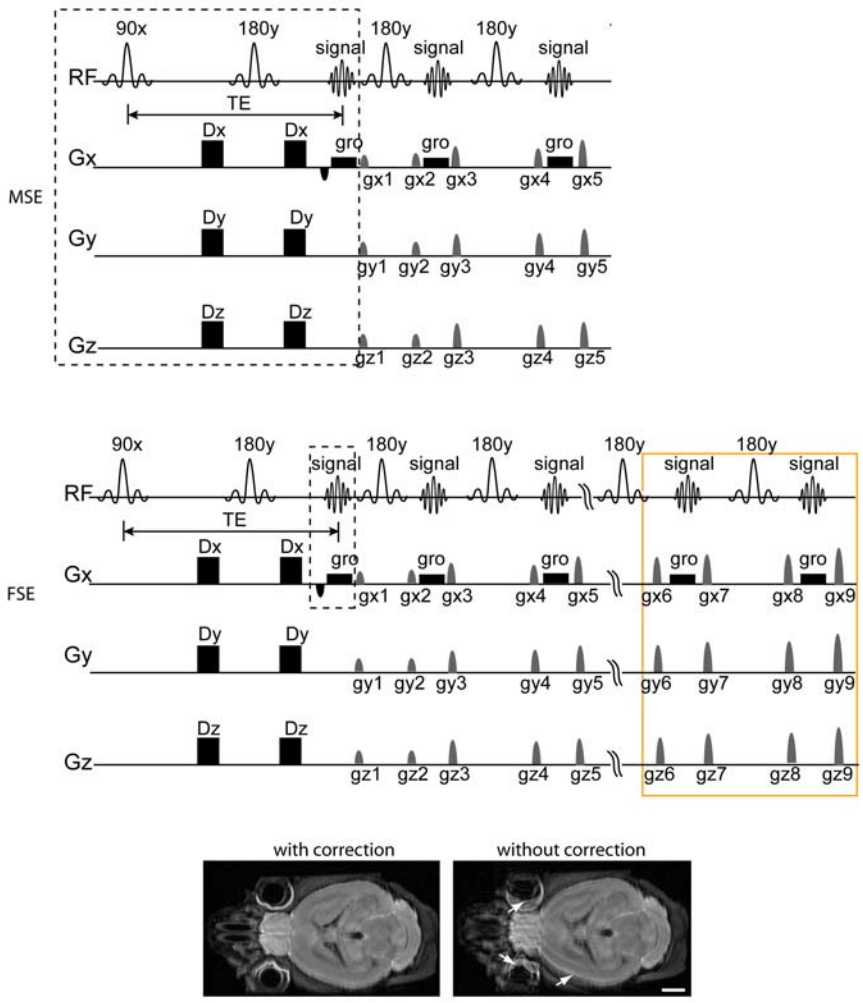

Figure 2: *Diagrams of multiple spin echo (MSE) and fast spin echo (FSE). In the diagrams, phase encoding gradients are not shown. Abbreviations are: Dx, Dy, and Dz: diffusion sensitizing gradients along the x, y, and z axes; gro: the read-out gradient; RF: radio frequency; Gx, Gy, and Gz: x, y, and z gradient axes; gx, gy, and gz: crusher gradients around the refocusing pulses along the x, y, and z axes. Inside the rectangular box of broken lines is the standard diffusion-weighted spin echo sequence. The part inside the orange box illustrates the twin-navigator echoes scheme. Diffusion-weighted mouse brain images with and without navigator correction are shown in the bottom. White arrows in the image without navigator correction indicate the artifacts caused by phase incoherence between echoes. These artifacts are removed using the twin-navigator correction scheme. Scale bars = 1 mm.*

Different combinations of diffusion times and *b* values have been used in DTI experiments. Diffusion time is a key parameter. Long diffusion time allows water molecules to fully explore their micro-environment. The dependence of measured diffusivity on diffusion time has been shown in muscle fibers [10]. In WM structures, because the diameter of each axon is much smaller than muscle fibers, such dependence disappeared when the diffusion time is larger than 5 ms [11]. Most studies used a diffusion time between 10 ms and 20 ms. The *b* value is another key parameter. Higher *b* values produce more diffusion weighted contrast but also reduce the SNR of the diffusion weighted image. Most *in vivo* studies used *b* values from 700 s/mm^2 to 1000 s/mm^2 for imaging mature brain and spinal cord. For *ex vivo* studies, because the diffusion coefficients in postmortem samples are lower than *in vivo [12]*, it is often necessary to increase the *b* value to 1500 – 2000 s/mm^2. For imaging immature brain and spinal cord, because the diffusivity is higher than mature brain and spinal cord, lower *b* values should be used.

In summary, we have presented the basic imaging sequences and parameters of mouse brain DTI. In practice, users will need to fine tune the sequence or parameters for particular hardware platforms or applications.

References:

1. Budde, M.D., et al., *Toward accurate diagnosis of white matter pathology using diffusion tensor imaging*. Magn Reson Med, 2007. **57**(4): p. 688-95.
2. Ahrens, E.T., et al., *MR microscopy of transgenic mice that spontaneously acquire experimental allergic encephalomyelitis.* Magn Reson Med, 1998. **40**(1): p. 119-32.
3. Sun, S.W., et al., *Noninvasive detection of cuprizone induced axonal damage and demyelination in the mouse corpus callosum.* Magn Reson Med, 2006. **55**(2): p. 302-8.
4. Sizonenko, S.V., et al., *Developmental changes and injury induced disruption of the radial organization of the cortex in the immature rat brain revealed by in vivo diffusion tensor MRI.* Cereb Cortex, 2007. **17**(11): p. 2609-17.
5. Tyszka, J.M., et al., *Statistical diffusion tensor histology reveals regional dysmyelination effects in the shiverer mouse mutant.* Neuroimage, 2006. **29**(4): p. 1058-65.
6. Mori, S., et al., *Diffusion tensor imaging of the developing mouse brain.* Magn Reson Med, 2001. **46**(1): p. 18-23.
7. Zhang, J., et al., *Three-dimensional anatomical characterization of the developing mouse brain by diffusion tensor microimaging.* Neuroimage, 2003. **20**(3): p. 1639-48.
8. Reese, T.G., et al., *Reduction of eddy-current-induced distortion in diffusion MRI using a twice-refocused spin echo.* Magn Reson Med, 2003. **49**(1): p. 177-82.
9. Mori, S. and P.C.M. van Zijl, *A motion correction scheme by twin-echo navigation for diffusion weighted magnetic resonance imaging with multiple RF echo acquisition.* Magn Reson Med, 1998. **40**: p. 511-516.
10. Kim, S., et al., *Dependence on diffusion time of apparent diffusion tensor of ex vivo calf tongue and heart.* Magn Reson Med, 2005. **54**(6): p. 1387-96.
11. Beaulieu, C., *The basis of anisotropic water diffusion in the nervous system - a technical review.* NMR Biomed, 2002. **15**(7-8): p. 435-55.
12. Sun, S.W., et al., *Differential sensitivity of in vivo and ex vivo diffusion tensor imaging to evolving optic nerve injury in mice with retinal ischemia.* Neuroimage, 2006. **32**(3): p. 1195-204.